12 Mar 1991, 10:30 am - 12:00 pm

Application of the Elastoplastic-Viscoplastic Bounding Surface Model to Cyclic Loading

Victor N. Kaliakin
University of Delaware, Newark, DE

Proceedings: Second International Conference on Recent Advances in Geotechnical Earthquake Engineering and Soil Dynamics, March 11-15, 1991, St. Louis, Missouri, Paper No. 1.31

Application of the Elastoplastic-Viscoplastic Bounding Surface Model to Cyclic Loading

Victor N. Kaliakin
Assistant Professor, Department of Civil Engineering, University of Delaware, Newark, DE 19716

SYNOPSIS: The predictive capabilities of the elastoplastic-viscoplastic bounding surface model, with emphasis on the response of cohesive soils subjected to cyclic loading, are discussed herein. This model, which represents a generalized three-dimensional constitutive formulation for isotropic cohesive soils, is developed within the framework of coupled elastoplasticity-viscoplasticity and critical state soil mechanics.

INTRODUCTION

In the past, limitations in analytical material descriptions, in laboratory testing and in computational capabilities imposed severe restrictions on attempts to model the complex behavior of soils. However, over the past few decades the development of high-speed computers and efficient numerical and experimental techniques has significantly reduced these limitations. As a result, much research in recent years has been directed towards the development of constitutive models possessing various levels of sophistication. Several of these models were developed within the framework of classical elastoplasticity. One shortcoming of such models is, however, their failure to accurately simulate the response of soils subjected to load reversals and to other complex quasi-static and dynamic loading histories. This shortcoming is primarily due to the inability of predicting irreversible inelastic deformation within the purely elastic region implicit in the concept of a yield surface. Thus, for correct simulation of response to complex loadings, new concepts must supplement the classical approach.

A very promising class of plasticity-based models, based on the notion of a bounding surface in stress space (Dafalias, 1975; Krieg, 1975), represent one such concept. The prominent feature of this concept is the fact that inelastic deformations can occur for stress points within or on a bounding surface in stress space at a pace depending on the proximity of the actual stress point to a properly defined "image" point on the surface itself. The image point is specified by an appropriate mapping rule which becomes the identity mapping if the stress state lies on the surface. The normal to the surface at the image point defines the direction of loading-unloading. At the image point a "bounding" plastic modulus is defined by means of the consistency condition for the bounding surface. The actual plastic modulus is a function of this bounding modulus and of the distance in stress space between the actual stress point and its "image" on the bounding surface. Thus, unlike classical yield surface plasticity, plastic states are not restricted only to those lying on a surface.

Following its original application to cohesive soils (Dafalias and Herrmann, 1980, 1982 a,b), the bounding surface model for cohesive soils was simplified (Kaliakin and Dafalias, 1989) and extended to account for time and rate effects (Kaliakin, 1985; Kaliakin and Dafalias, 1990a). This latter model is a generalized three-dimensional formulation developed within the framework of coupled elastoplasticity-viscoplasticity (Dafalias, 1982) and critical state soil mechanics (Schofield and Wroth, 1968); a microscopic basis for the model is presented in (Dafalias, 1982; Kaliakin, 1985). The notion of such a soil model differs from classical yield surface elastoplasticity–viscoplasticity formulations in that the stress is assumed to be continuously at an inelastic state, with the possibility of plastic-viscoplastic coupling, either within or on the bounding surface. Furthermore, unlike some other time dependent formulations (Adachi and Oka, 1982; Nova, 1982; Oka, 1985; Sekiguchi, 1984), this model is not restricted to normally consolidated cohesive soils, but is capable of describing the material response at any overconsolidation ratio (OCR), for soils subjected to either monotonic or cyclic loading. The model thus represents a novel approach to simulating the time related behavior of soils. Following its implementation into several computer codes (Herrmann and Kaliakin, 1987; Kaliakin and Herrmann, 1987), the present model was extensively verified. Its application to normally-, lightly-, and heavily overconsolidated soils subjected to monotonic and cyclic loading under drained and undrained conditions has agreed quite favorably with experimental results (Kaliakin, 1988; Kaliakin and Dafalias, 1989, 1990b) and with actual field measurements (Poran et al. 1986; Kaliakin et al. 1990).

The purpose of this paper is to present the predictive capabilities of the elastoplastic-viscoplastic bounding surface model, with emphasis on the response of cohesive soils subjected to cyclic loading. Like previous bounding surface models for cohesive soils, the present formulation successfully predicts the following phenomena:

1) For normally or lightly consolidated soils the model predicts: positive pore pressure build-up, axial strain accumulation and reduction of effective stress under undrained conditions, and the accumulation of volumetric and deviatoric strain under drained conditions;

2) For heavily overconsolidated soils the model predicts: the build-up of negative pore pressure under undrained conditions, and the accumulation of dilative volumetric strain under drained conditions;

3) The stabilization of stress-strain loops under small amplitudes of cyclic deviatoric stress; and,

4) The progressive evolution of the material state toward the critical state (where failure is imminent) under large amplitudes of cyclic deviatoric stress.

Unlike previous presentations of cyclic bounding surface response which were primarily qualitative in nature (Dafalias and Herrmann, 1980; 1982 a,b; Dafalias et al. 1981), the present assessment involves the comparison of numerical results with those measured in the laboratory. It is important to point out that within the context of the present model, cyclic loading is viewed as nothing more than a sequence of monotonic loadings (of differing sign) which alter the degree of overconsolidation of the soil. Since the model is capable of predicting the response of soils at any OCR, it is not surprising that success in predicting cyclic response is achieved.

FORMULATION FOR ISOTROPIC COHESIVE SOILS

The elastoplastic-viscoplastic bounding surface formulation is completely general in nature (Kaliakin and Dafalias, 1990a). For brevity in the present development, only an overview of the formulation – specialized for isotropic cohesive soils – is given. Tensors are presented in indicial form following the summation convention over repeated indices. Compressive stresses and strains are positive, and only small deformations are considered.

The material is defined in terms of the effective stress tensor σ_{ij} and a single internal variable which accounts for the nonconservative nature of soil by keeping track of the past loading history. The dependence of the bounding surface on σ_{ij} is expressed in terms of the following three stress invariants:

$$I = \sigma_{kk}\,, \quad J = \sqrt{\frac{1}{2}\, s_{ij}\, s_{ij}}\,, \quad \alpha = \frac{1}{3}\sin^{-1}\left[\frac{\sqrt{3}}{2}\left(\frac{s_{ij}\, s_{jk}\, s_{ki}}{J^3}\right)\right] \qquad (1)$$

where s_{ij} and α ($-\pi/6 \le \alpha \le \pi/6$) represent the deviatoric part of σ_{ij} and the "Lode" angle, respectively. A meridional section of the surface (i.e., for a given value of α) is shown in Fig. 1.

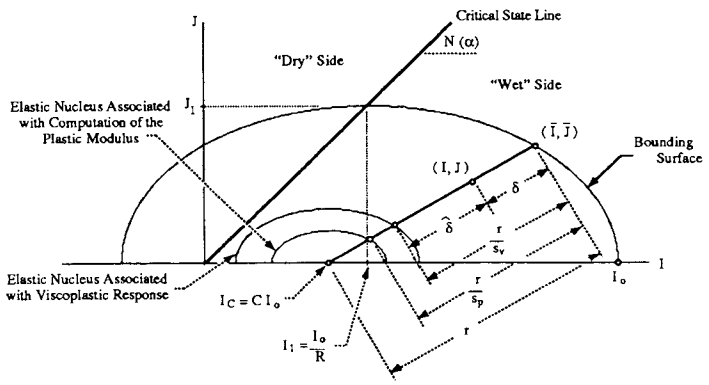

Fig. 1. Schematic Illustration of the Radial Mapping Rule and of the Bounding Surface in Stress Invariants Space

The actual stress point (I, J) is related to its "image" value $(\bar{I}, \bar{J})$ on the bounding surface itself through a "radial mapping" rule (Dafalias and Herrmann, 1986) which is analytically expressed by

$$\bar{I} = b\,(I - CI_o) + CI_o\,, \quad \bar{s}_{ij} = b\, s_{ij} \quad \Rightarrow \quad \bar{J} = J\,, \quad \bar{\alpha} = \alpha \qquad (2)$$

where C represents a model parameter ($0 \le C < 1$), $1 \le b \le \infty$, and I_o represents the intersection of the bounding surface with the positive I-axis. Using CI_o as the projection center (Fig. 1), the image stress is obtained by the radial projection of the actual stress onto the bounding surface (hence the name "radial mapping").

Denoting the infinitesimal strain tensor by ε_{ij} and its elastic, viscoplastic, and plastic components by the superscripts e, v, and p, respectively, the following linear decomposition is assumed:

$$\dot{\varepsilon}_{ij} = \dot{\varepsilon}^{e}_{ij} + \dot{\varepsilon}^{v}_{ij} + \dot{\varepsilon}^{p}_{ij} \qquad (3a)$$

$$= C_{ijkl}\,\dot{\sigma}_{kl} + \langle\phi\rangle\frac{\partial F}{\partial \bar{\sigma}_{ij}} + \langle L\rangle\frac{\partial F}{\partial \bar{\sigma}_{ij}} \qquad (3b)$$

where a dot indicates a rate (material time derivative) and an associated flow rule is assumed. In Eq. (3b) the symbols $\langle\ \rangle$ denote the Macaulay brackets, $F = 0$ represents the analytical expression of the bounding surface, and C_{ijkl} denotes the fourth order tensor of elastic compliance. The direction of the plastic strain rate, as well as that of the loading/unloading (associated flow rule), is given by

$$\frac{\partial F}{\partial \bar{\sigma}_{ij}} = F_{,\bar{I}}\,\delta_{ij} + \frac{F_{,\bar{J}}\, s_{ij}}{2J} + \frac{\sqrt{3}\, F_{,\alpha}}{2bJ\cos 3\alpha}\left[\frac{1}{J^2}\left(s_{ik}\, s_{kj} - \frac{3}{2}\frac{S^3\, s_{ij}}{J^2}\right) - \frac{2}{3}\delta_{ij}\right] \qquad (4)$$

where a comma indicates partial differentiation with respect to the index which follows. The viscoplastic effects, which are based upon a generalization of Perzyna's theory (Perzyna, 1966), enter the formulation through the scalar "overstress" function ϕ, where

$$\phi = \frac{1}{V}\exp\left(\frac{J}{NI}\right)\left(\frac{\hat{\delta}}{r - \frac{r}{s_v}}\right)^n \qquad (5)$$

The "distances" $\hat{\delta}$ and r, and the critical state line slope N are shown in Fig. 1. The quantities s_v, V and n represent model parameters to be discussed subsequently. In Eq. (3b) the quantity L represents a scalar loading index (loading, neutral loading, and unloading occur when $L > 0$, $L = 0$ and $L < 0$, respectively). A key step in developing the present formulation is the proper definition of L to account for the coupling of plastic-viscoplastic hardening for states on and within the bounding surface. Within the framework of the radial mapping rule and for the special case of isotropic cohesive soils, L is defined by (Kaliakin and Dafalias, 1990a):

$$L = \frac{1}{K_p}\left\{F_{,\bar{I}}\,\dot{I} + F_{,\bar{J}}\,\dot{J} + \frac{1}{b}F_{,\alpha}\,\dot{\alpha} - \langle\phi\rangle\bar{K}_p\left[\frac{1}{b} - C\left(1 - \frac{1}{b}\right)\frac{F_{,\bar{I}}}{F_{,I_o}}\right]\right\}$$
$$= \frac{1}{\bar{K}_p}\left\{F_{,\bar{I}}\,\dot{\bar{I}} + F_{,\bar{J}}\,\dot{\bar{J}} + F_{,\alpha}\,\dot{\bar{\alpha}}\right\} - \langle\phi\rangle \qquad (6)$$

The quantity K_p represents the plastic modulus associated with the actual stress state; $\bar{K}_p$ represents the "bounding" plastic modulus associated with the "image" stress state (i.e., for $b = 1$). A general expression for $\bar{K}_p$ is obtained by means of the consistency condition for the surface; i.e., $\dot{F} = 0$. The feature which distinguishes the present formulation from classical elastoviscoplasticity formulations is that K_p is obtained not from a consistency condition, but from the following relation which depends upon $\bar{K}_p$ and upon the distances δ and r (Fig. 1):

$$K_p = \bar{K}_p + H \frac{\delta}{\langle r - s_p \delta \rangle} \tag{7}$$

In the above expression H represents the "shape hardening" function which defines the shape of stress-strain curves during inelastic hardening (or softening) for points within the bounding surface (Kaliakin and Dafalias, 1989).

In Eq. (7) the quantity s_p represents an "elastic nucleus" parameter (Fig. 1) whose incorporation into the formulation facilitates predictions under cyclic conditions. By considering the material response implied by Eq. (7), a better insight into the definition of this elastic nucleus can be obtained. When $\delta = 0$, the actual and image stress points coincide and $K_p = \bar{K}_p$. For $0 < \delta < r/s_p$ the actual stress point lies in the space between the bounding surface and the elastic domain and $K_p > \bar{K}_p$ (with $K_p \rightarrow \infty$ continuously as $\delta \rightarrow r/s_p$). Finally, for all $\delta \geq r/s_p$ the Macaulay bracket in Eq. (7) yields zero, rendering K_p infinite and, therefore, defining a purely elastic range around the projection center CI_o(Fig. 1). This range is the elastic nucleus. A stress state moving from within the elastic nucleus crosses its boundary and moves outside with a smooth elastoplastic transition at $\delta = r/s_p$ according to Eq. (7). Thus, although the boundary of the elastic nucleus is equivalent to the concept of a yield surface, it is not identical since the stress point does not necessarily stay on it; i.e., no consistency condition is required for the elastic nucleus. The effect of the size of the elastic nucleus on cyclic model predictions has been discussed in detail by Dafalias et al. (1981). As such, only a brief overview is presented herein. Consider the case of cyclic response under undrained triaxial conditions. Let p (= I/3) and q ($= \pm \sqrt{3}$ J) denote the mean normal effective stress and the principal stress difference, respectively. If $s_p = 1.0$, the elastic nucleus shrinks to a point (the projection center CI_o shown in Fig. 1); with repeated loading at any level of q, the undrained stress paths will move toward failure at the critical state line (Fig. 1) and will be accompanied by an increase in pore pressure. If $s_p > 1.0$ and the magnitude of q is low, the stress point will enter the elastic nucleus. At this point fully elastic response will be predicted, resulting in full stabilization. If the magnitude of q is large, the stabilization will occur at a slower rate. Furthermore, if the size of the elastic nucleus is reduced (by decreasing $s_p \rightarrow 1.0$), and the magnitude of q is large, the stress point may reach the critical state line thus leading to the prediction of failure. From this brief description it is evident that through the presence of the elastic nucleus, realistic predictions of cyclic response (including stabilization and/or failure at the critical state) can indeed be realized. This is especially true when such predictions are compared to those associated with classical yield surface elastoplasticity-based formulations, for the latter would predict an initial p-q loop with immediate stabilization.

The bounding surface is assumed to undergo isotropic hardening. The hardening is controlled by a single scalar internal variable which measures the inelastic volumetric strain ε^i_{kk}. This variable is defined as the inelastic rate of the total void ratio e, given by

$$\dot{e}^i = -(1 + e_{in})\, \dot{\varepsilon}^i_{kk} \tag{8}$$

where e_{in} represents the initial void ratio corresponding to the reference configuration with respect to which engineering strains are measured. For natural strains, e must be substituted for e_{in} in Eq. (8) as well as in all subsequent expressions. The dependence of the bounding surface on ε^i_{kk} is assumed to occur only through the dependence of I_o on ε^i_{kk}. Since material isotropy is assumed, I_o is thus a measure of preconsolidation history. Assuming linear e-ln I consolidation and swelling relations (Schofield and Wroth, 1968) it follows that the hardening behavior of the bounding surface is analytically described by:

$$\frac{dI_o}{de^i} = -\frac{\langle I_o - I_L \rangle + I_L}{\lambda - \kappa} \tag{9}$$

where the critical state parameters λ and κ represent the slopes, in e-ln I space, of the virgin consolidation and swell/recompression lines, respectively, for either isotropic or anisotropic consolidation. It follows also that

$$\frac{dI}{de^e} = -\frac{\langle I - I_L \rangle + I_L}{\kappa} \tag{10}$$

The transitional stress I_L appearing in Eqs. (9) and (10) represents the value of I and/or I_o below which the relation between I or I_o and void ratio changes smoothly from logarithmic to linear. I_L is not related to the bounding surface concept and was introduced into the formulation to prevent excessive softening from occurring for small values of I (or I_o). In the majority of applications involving the bounding surface model (including the one discussed herein), I_L has been set equal to the atmospheric pressure. Noting that $\dot{e}^e = -(1 + e_{in})\, \dot{\varepsilon}^e_{kk}$, and using Eq. (10) in conjunction with the relationship $\dot{I} = \dot{\sigma}_{kk} = 3K\, \dot{\varepsilon}^e_{kk}$, yields the following expression for the elastic bulk modulus K:

$$K = \frac{(1 + e_{in})(\langle I - I_L \rangle + I_L)}{3\kappa} \tag{11}$$

It is evident that were it not for the presence of I_L, K would equal zero for I = 0.

After suitable manipulation, the constitutive relations, in inverse form, are given by

$$\dot{\sigma}_{ij} = D_{ijkl}\, \dot{\varepsilon}_{kl} - V_{ij} \tag{12}$$

Explicit expressions for the fourth rank incremental stiffness tensor D_{ijkl} and for the second rank tensor of viscoplastic contribution V_{ij} are given in (Kaliakin and Dafalias, 1990b).

A SPECIFIC FORM OF THE BOUNDING SURFACE

The bounding surface is explicitly defined by

$$F = (\bar{I} - I_o)\left(\bar{I} + \frac{R-2}{R} I_o\right) + (R-1)^2 \left(\frac{\bar{J}}{N}\right)^2 = 0 \tag{13}$$

where R represents a constant model parameter which completely defines the shape of this elliptical surface (Fig. 1). The slope of the critical state line (CSL) in stress invariants space is defined by N, which

is a function of the third stress invariant. The CSL intersects the bounding surface at the point $(I_1, J_1) = (I_o/R, J_1)$ where, as required, $F,_{\bar{I}} = 0$.

IDENTIFICATION AND DETERMINATION OF PARAMETERS

Associated with the most general form of the model are fifteen parameters, the values of which fall within fairly narrow ranges and are determined using a well-defined calibration procedure (Kaliakin and Dafalias, 1987). With a single set of parameter values the model predicts the behavior of soils at any OCR, subjected to either monotonic or cyclic compression and/or extension loading under either drained or undrained conditions.

Elastoplastic Model Parameters

The values of the twelve parameters in this category are determined by matching the results of standard laboratory experiments of duration short enough to ensure negligible viscoplastic effects. The traditional material constants include the elastic shear modulus G (or, alternatively, Poisson's ratio ν) and the critical state parameters λ, κ and M (the values of M associated with triaxial compression and extension are denoted by M_c and M_e, respectively; M is related to N through $M = 3\sqrt{3}\ N$). The elastic bulk modulus K is defined in terms of κ and I by means of Eq. (11), and G is either determined explicitly or is computed from κ and a constant ν (in the latter case, G is a function of I and consequently invalidates the existence of an elastic potential). The surface configuration parameters consist of the shape parameter R (Eq. 13), the elastic zone parameter s_p (Eq. 7), and the projection center parameter C (Eq. 2). In the current formulation different elastic nuclei are assumed for purposes of computing ϕ (Eq. 5) and K_p (Eq. 7). Since both nuclei have the projection center as their center of homology (Fig. 1), it follows that the selection of C influences the magnitude of both quantities. The hardening parameters h_c, h_e, "a" and "w" enter the expression for K_p (Eq. 7) through the function H (Kaliakin and Dafalias, 1989); they control the degree of plastic hardening (or softening) that occurs at stress states within the bounding surface. With the possible exception of C, the elastoplastic parameters are inactive during the determination of values for the viscoplastic parameters.

Viscoplastic Model Parameters

The viscoplastic contribution enters the constitutive relations through the continuous scalar overstress function ϕ (Eq. 5). The viscoplastic model parameters, which are determined by matching the results of at least one long term laboratory experiment, include the viscoplastic zone parameter s_v ($1 < s_v < \infty$), and the parameters V and n. Suitable values for s_v (and possibly for C) are determined by matching predicted values of the maximum change in I (and thus in the pore pressure) with those observed experimentally. This determination is performed independent of the values of the remaining viscoplastic parameters (Kaliakin and Dafalias, 1990a). Increases in s_v enlarge the elastic nucleus (Fig. 1), reduce the value of $\hat{\delta}$ and thus slow the viscoplastic evolution of the bounding surface (and the pore pressure build-up and the axial strain development under conditions of undrained creep). An increase in C results in the movement of the projection center to larger positive values of I (Fig. 1). This has nearly the same effect on the predictions as does an increase in s_v. However, both parameters are typically necessary in order to accurately predict time dependent response of the material. Finally, values for the parameters V and n are determined by matching the predicted pore pressure– and axial strain time histories (Kaliakin and Dafalias, 1990a) with those observed experimentally. For relatively small values of V the response is nearly inviscid throughout the loading history; i.e., the viscous response occurs very rapidly. If, on the other hand, V is large, the viscoplastic strain is greatly reduced, resulting in little change in the overall response with time. Increases in n have a similar effect on the response as do increases in V, though variations in the latter have a greater influence on the initial slope of the response curves.

VERIFICATION OF THE MODEL

To verify the adequacy of the model, the constitutive equations, along with such enhancements as local iteration, sub-stepping and radial return, were incorporated into a modular system of FORTRAN 77 subroutines (Herrmann et al. 1987). The modular design facilitates simple and inexpensive incorporation of the subroutines into new and existing programs for the analysis of earth structures (Herrmann and Kaliakin, 1987; Kaliakin and Herrmann, 1987).

Simulation Of Cyclic Undrained Triaxial Response

The results of cyclic strain-controlled undrained triaxial tests performed on saturated, artificially prepared clay specimens were reported by Taylor and Bacchus (1969). The tests employed different axial strain (ε_1) levels which were applied to specimens possessing various levels of overconsolidated. In each test one-hundred strain cycles of constant amplitude were applied to a specimen at a frequency of 0.2 cycles per second. In addition to the aforementioned cyclic tests a series of "static" tests (involving only one-quarter of a cycle of loading) were performed.

For purposes of calibrating the model parameters, values for e_{in} and for the traditional material constants ($\lambda = 0.142$, $\kappa = 0.022$, and $M_c = 1.50$) were determined directly from figures 2 and 10 in Taylor and Bacchus (1969). The equation

$$M_c = \frac{6 \sin \phi'}{3 - \sin \phi'} \tag{14}$$

was next solved for the effective friction angle ϕ'. Substituting this value into the equation

$$M_e = \frac{6 \sin \phi'}{3 + \sin \phi'} \tag{15}$$

yielded a value of $M_c = 1.00$. A value of $\nu = 0.20$ was assumed based on the response shown in Fig. 9 of Taylor and Bacchus (1969). Next a value for the shape parameter R (=2.10) was determined by matching the experimental undrained stress path for a "static" test performed on a normally consolidated (OCR = 1.0) specimen. A comparison of the numerical simulations (shown in the form of continuous curves) and the experimental results (depicted by discrete symbols) for this test is presented in Figs. 2 and 3. The location of the projection center, described by the value of the projection center parameter C (= 0.25), was fixed based on the shapes of the undrained stress paths associated with overconsolidated specimens tested under static conditions (Kaliakin and Dafalias, 1987). Values for the hardening parameters h_c (= 1.0), h_e (= 1.0), a (= 1.2), and w (= 5.0) were set equal to commonly used values (Kaliakin and Dafalias, 1987). As it turned out, during the course of the model calibration these parameter values did not need to be adjusted.

Since the frequency of loading was fairly high, viscoplastic effects did not have a chance to become manifest. As such, the viscoplastic model parameters s_v, V and n were set equal to arbitrary, though representative values (Kaliakin and Dafalias, 1987). Finally, a suitable value for the elastic nucleus parameter s_p (=1.80) was determined by matching the experimental results at various levels of cyclically applied axial strain.

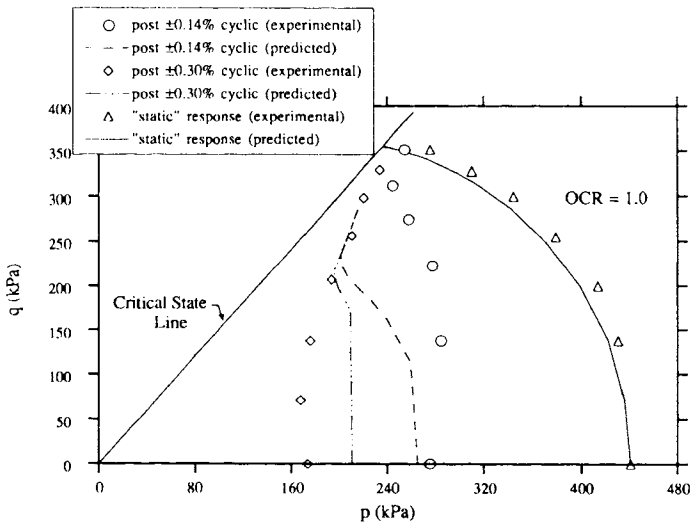

Fig. 2. Undrained Stress Paths for "Static" Test and for Strength Tests After Cyclic Loading

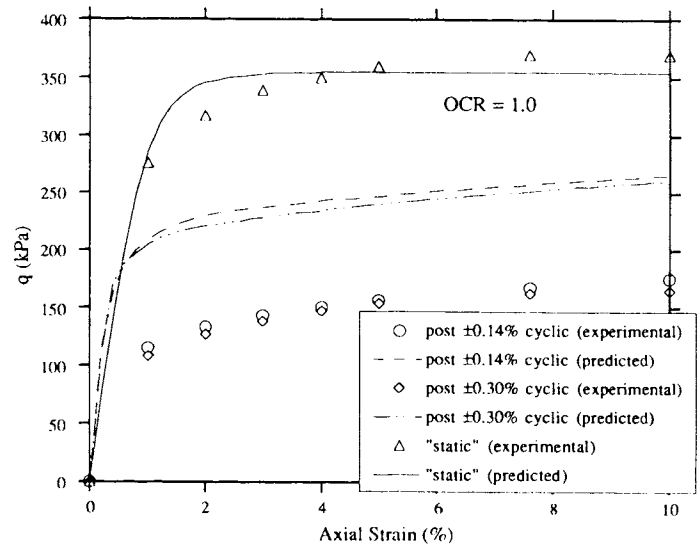

Fig. 3. Stress-Strain Response for "Static" Test and for Strength Tests After Cyclic Loading

The simulated undrained stress paths associated with $\varepsilon_1 = \pm 0.14\%$ and $\varepsilon_1 = \pm 0.30\%$ are shown in Figs. 4 and 5, respectively. In these figures the numerical predictions are represented by continuous curves; the associated experimental points are depicted by discrete symbols with a label indicating the number of cycles at which this reading was taken. As evident from Figs. 4 and 5, the reduction in p with progressive cyclic loading has been over- and under-predicted, respectively. This is explained by the fact that but a single parameter (s_p) is used to define the size of the elastic nucleus. As such, a compromise must typically be reached. The levels of q shown in Figs. 4 and 5 were over-predicted. This is explained by the fact that with each loading cycle the bounding surface expands and the plastic modulus K_p increases in magnitude. As a result, only a very small amount of inelastic strain is predicted during each cycle. In actual laboratory experiments the material stiffness is, however, known to progressively degrade. This phenomenon can easily be accounted for in the present model by introducing a degradation ("damage") term. This, however, necessitates the addition of two extra model parameters and complicates the formulation. As such, the simulation of material degradation was not further pursued herein. Additional details regarding this subject are found in Dafalias et al. (1982).

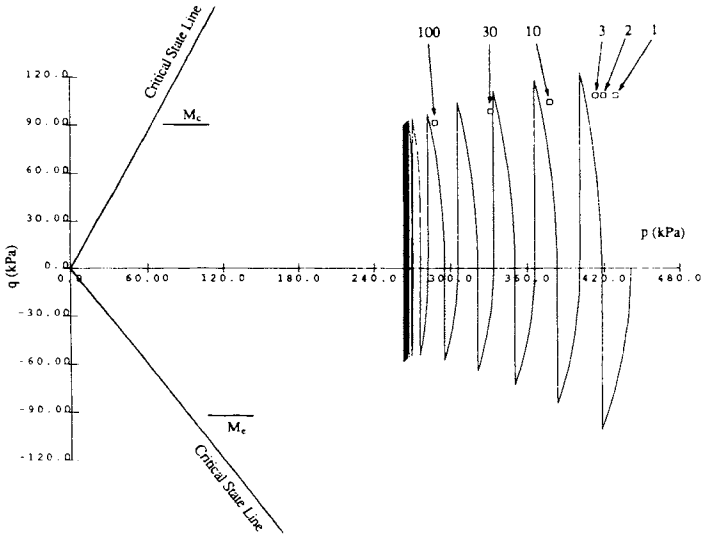

Fig. 4. Simulated Undrained Stress Paths Associated with Cyclic Loading of ±0.14% Axial Strain

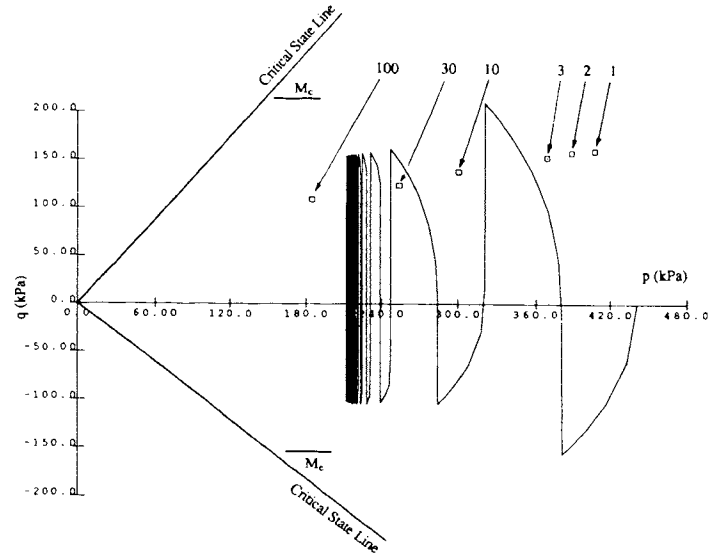

Fig. 5. Simulated Undrained Stress Paths Associated with Cyclic Loading of ±0.30% Axial Strain

As a final assessment of the predictive capabilities of the present bounding surface model, the undrained response following cyclic loading was investigated. This involved the simulation of a monotonic strain-controlled shearing following the one-hundredth loading cycle. At the end of cyclic loading the material is moderately to heavily overconsolidated. Realistic prediction of post-cyclic shearing thus requires the capability of simulating response at any OCR – one of strengths of the present model. The numerical simulations of post-cyclic undrained shearing are shown in Figs. 2 and 3. It is evident that due to the lack of accurate prediction of the decrease in p, the initial portion of the post-cyclic undrained stress paths differs from the experimental values (Fig. 2). The agreement improves with increasing values of q, particularly for $\varepsilon_1 = \pm 0.30\%$. The stress-strain response shown in Fig. 3 shows a substantial discrepancy between experimental and numerical results. This is largely due to the aforementioned failure of accounting for material degradation.

CONCLUSION

This paper has focused on the cyclic predictions generated by the elastoplastic-viscoplastic bounding surface model. This model is a generalized, three-dimensional formulation based on the concept of a bounding surface in stress space and developed within the framework of coupled elastoplasticity-viscoplasticity and critical state soil mechanics. Within the context of the present model cyclic loading is viewed as a sequence of monotonic loadings of differing sign which alter the degree of overconsolidation of the material. Since the model is capable of predicting the response of cohesive soils at any OCR, it is not surprising that success in predicting cyclic response is achieved. The numerical simulations presented herein tend to support this notion. The discrepancies between numerical and experimental results have been identified and remedies for alleviating them have been discussed.

REFERENCES

Adachi, T. and Oka, F., "Constitutive Equations for Normally Consolidated Clay Based on Elasto-Viscoplasticity", Soils and Foundations, 22, No. 4, 1982, 57-70.

Dafalias, Y. F., "On Cyclic and Anisotropic Plasticity: i). A General Model Including Material Behavior under Stress Reversals, ii). Anisotropic Hardening for Initially Orthotropic Materials," Ph. D. dissertation presented to the University of California, Berkeley, 1975.

Dafalias, Y. F., and Herrmann, L. R., "A Bounding Surface Soil Plasticity Model," Proc. Int. Symp. on Soils Under Cyclic and Transient Loading, G. N. Pande and O. C. Zienkiewicz eds., A. A. Balkema, pub., Rotterdam, 1980, 335-345.

Dafalias, Y. F., Herrmann, L. R., and Anandarajah, A., "Cyclic Loading Response of Cohesive Soils Using a Bounding Surface Plasticity Model," Proc. International Conference on Recent Advances in Geotechnical Earthquake Engineering and Soil Dynamics, St. Louis, Mo., vol. 1, 1981, 139-144.

Dafalias, Y. F., and Herrmann, L. R., "Bounding Surface Formulation of Soil Plasticity," Ch. 10 in: Soil Mechanics – Transient and Cyclic Loads, G. N. Pande and O. C. Zienkiewicz eds., J. Wiley and Sons, Inc., pub., Chichester, U. K., 1982a, 253-282.

Dafalias, Y. F., and Herrmann, L. R., "A Generalized Bounding Surface Constitutive Model for Clays," Application of Plasticity and Generalized Stress-Strain in Geotechnical Engineering, R. N. Yong and E. T. Selig eds., pub. by ASCE, New York, 1982b, 78-95.

Dafalias, Y. F., "Bounding Surface Elastoplasticity - Viscoplasticity for Particulate Cohesive Media," Deformation and Failure of Granular Materials, P. A. Vermeer and H. J. Luger, eds., A. A. Balkema, pub., Rotterdam, 1982, 97-107.

Dafalias, Y. F., Herrmann, L. R., and DeNatale, J. S., "The bounding surface plasticity model for isotropic cohesive soils and its application at the Grenoble workshop," Results of the International Workshop on Constitutive Relations for Soils, Gudehus, et al. eds., Balkema pub., Grenoble, 1982, 273-287.

Dafalias, Y. F., and Herrmann, L. R., "Bounding Surface Plasticity II: Application to Isotropic Cohesive Soils," Journal of Engineering Mechanics, ASCE, vol. 112, no. 12, 1986, 1263-1291.

Herrmann, L. R., and Kaliakin, V. N., "User's Manual for SAC-2, A Two-Dimensional Nonlinear, Time Dependent, Soil Analysis Code Using the Bounding Surface Elastoplasticity–Viscoplasticity Model," Volumes I and II, Department of Civil Engineering Report, University of California, Davis, 1987.

Herrmann, L. R., Kaliakin, V. N., Shen, C. K., Mish, K. D., and Zhu, Z-Y, "Numerical Implementation of a Plasticity Model for Cohesive Soils," Journal of Engineering Mechanics, ASCE, vol. 113, no. 4, 1987, 500-519.

Kaliakin, V. N., "Bounding Surface Elastoplasticity-Viscoplasticity for Clays," Ph. D. dissertation presented to the University of California, Davis, 1985.

Kaliakin, V. N., and Herrmann, L. R., "Numerical Implementation of the Elastoplastic–Viscoplastic Bounding Surface Model for Isotropic Cohesive Soils – The EVALVP Computer Program," Department of Civil Engineering Report, University of California, Davis, 1987.

Kaliakin, V. N., and Dafalias, Y. F., "Details Regarding the Elastoplastic-Viscoplastic Bounding Surface Model for Isotropic Cohesive Soils," Department of Civil Engineering Report, University of California, Davis, December 1987.

Kaliakin, V. N., "An Elastoplastic-Viscoplastic Bounding Surface Model for Isotropic Cohesive Soils," International Conference on Rheology and Soil Mechanics, M. J. Keedwell, ed., Elsevier Applied Science, pub., 1988, 147-163.

Kaliakin, V. N. and Dafalias, Y. F., "Simplifications to the Bounding Surface Model for Cohesive Soils," International Journal for Numerical and Analytical Methods in Geomechanics, vol. 13, no. 1, 1989, 91-100.

Kaliakin, V. N. and Dafalias, Y. F., "Theoretical Aspects of the Elastoplastic-Viscoplastic Bounding Surface Model for Cohesive Soils," Soils and Foundations, vol. 30, no. 3, 1990a.

Kaliakin, V. N. and Dafalias, Y. F., "Verification of the Elastoplastic-Viscoplastic Bounding Surface Model for Cohesive Soils," Soils and Foundations, vol. 30, no. 3, 1990b.

Kaliakin, V. N., Muraleetharan, K. K., Dafalias, Y. F., Herrmann, L. R., and Shinde, S. B., "Foundation-Response Predictions Below Caisson-Retained Island," Journal of Geotechnical Engineering, ASCE, vol. 116, no. 9, 1990, 1291-1308.

Krieg, R. D., "A Practical Two-Surface Plasticity Theory," J. App. Mech., ASME, vol. 98, no. 4, 1975, 641-646.

Nova, R., "A Viscoplastic Constitutive Model for Normally Consolidated Clay", Deformation and Failure of Granular Materials, P. A. Vermeer, and H. J. Luger, eds., A. A. Balkema, pub., Rotterdam, 1982, 287-295.

Oka, F., "Elasto/Viscoplastic Constitutive Equations with Memory and Internal Variables", Computers and Geotechnics, vol. 1, 1985, 59-69.

Perzyna, P., "Fundamental Problems in Viscoplasticity", Adv. in Applied Mech., vol. 9, 1966, 243-377.

Poran, C. J., Kaliakin, V. N., Herrmann, L. R., Romstad, K. M., Lee, D.-F., and Shen, C. K., "Prediction of Trial Embankment Behavior Hertfordshire County Councils – Stansford Abbotts", Proceedings of the Reinforced Embankment on Soft Ground, King's College, London, September 1986.

Sekiguchi, H., "Theory of Undrained Creep Rupture of Normally Consolidated Clay Based on Elasto-Viscoplasticity", Soils and Foundations, vol. 24, no. 1, 1984, 129-147.

Schofield, A. N., and Wroth, C. P., Critical State Soil Mechanics, McGraw-Hill, London, 1968.

Taylor, P. W. and Bacchus, D. R., "Dynamic Cyclic Strain Tests on a Clay", Proc. 7th International Conference on Soil Mechanics and Foundation Engineering, Mexico City, 1969, vol. 1, 401-409.